Transition Measurements of a Micron-Sized Transition-Edge Hot-Electron Microbolometer

E.M. Barrentine[a], D.E. Brandl[a], A.D. Brown[b], N.T. Cao[b], K.L. Denis[b,c], W.T. Hsieh[b], T.R. Stevenson[b], P.T. Timbie[a], K. U-Yen[b] and E.J. Wollack[b]

[a]*University of Wisconsin-Madison, Madison, WI 53706 USA*
[b]*NASA Goddard Space Flight Center, Greenbelt, MD 20771 USA*
[c]*MEI Technologies Inc., Seabrook, MD 20706 USA*

Abstract. We are developing a Transition-Edge Hot-electron Microbolometer (THM) for use in large detector array applications in millimeter-wave astronomy. This bolometer detector consists of a superconducting bilayer TES with an overlapping thin-film semi-metal absorber. The detector is deposited directly on the substrate and thermal isolation of the bolometer is controlled by electron-phonon scattering within the small volume of the detector. We present measurements characterizing the transition behavior of several micron-sized THM test devices which are optimized for photon-noise-limited observations of the Cosmic Microwave Background (CMB). We interpret these measurements in terms of a lateral proximity effect between the TES and the superconducting Nb TES leads. We discuss possible modifications to the THM design to compensate for this effect while retaining the small detector volume necessary to obtain the desired value of electron-phonon thermal conductivity.

Keywords: Bolometers, hot-electron, Millimeter wave detectors, superconducting sensors, proximity effect
PACS: 07.57.Kp

INTRODUCTION

The Transition-edge Hot-electron Microbolometer (or THM) is a bolometric detector that measures incoming power by monitoring the temperature of an antenna-coupled absorber. A sensitive voltage-biased superconducting bilayer Transition-Edge Sensor (TES) is used as the thermometer with a SQUID ammeter to read out the temperature-dependent TES current.

The THM has applications to millimeter and submillimeter astronomy. In particular we are developing the detector for use in large detector arrays for measurements of the Cosmic Microwave Background (CMB) polarization signal. These large arrays of 1000s of detectors are needed in the search for the faint imprint of gravitational waves from the inflation era[1].

Unlike membrane-isolated bolometers which use micromachined structures to control the thermal conductance of the bolometer, the THM is deposited directly on the substrate. The design is similar to another hot-electron detector design[2] but includes a separate absorber as shown in Figure 1. The thermal conductance of the THM, when operating at low temperatures and with high electron-electron thermal conductance, is dominated by electron-phonon scattering between the "hot" electrons in the detector and the cooler phonons in the detector and substrate.

The electron-phonon thermal conductance has been shown to exhibit a power-law dependence on temperature, T, and a linear dependence on the detector volume, where $G_{e-p} = 5V\Sigma T^4$.[3,4] Here V is the volume and Σ is a material-dependent constant. When voltage-biased in the transition, $T = T_c$.

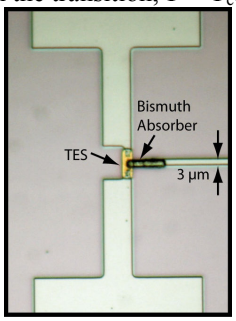

FIGURE 1. An optical image of a 3 μm x 3 μm TES with absorber. The microwave signal is transmitted from the right on a Nb microstripline terminating on the absorber which overlaps the Mo/Au TES. A Nb microwave termination structure[4] also overlaps the bilayer TES and serves as the DC leads to the TES.

CP1185, *Low Temperature Detectors LTD 13, Proceedings of the 13th International Workshop*
edited by B. Cabrera, A. Miller, and B. Young

For optimal thermal noise performance of the THM detector (in our case, below photon-noise-limited levels for CMB observation) the thermal conductance and temperature of the bolometer are optimized by controlling both geometry and T_c. A detailed account of the optimization of the THM detector under various background loadings has been given previously[5].

The transition temperature of a bilayer TES is tailored using a proximity effect in which the T_c and transition width of a thin superconducting film are modified by the presence of a thin normal metal film deposited on top of the superconductor[6]. A similar effect can also occur in the lateral direction between the bilayer TES and the superconducting Nb leads[7-10].

The physical interpretation of this lateral proximity effect is that the superconducting Cooper pairs in the leads retain their coherence as they travel a finite distance into the normal (or transitioning) metal. Over this distance the metal exhibits the zero-resistance properties of a superconductor. The length at which Cooper pairs retain coherence is characterized by the normal metal coherence length given by $\varepsilon_n = \sqrt{\frac{\hbar D}{2\pi k_B T}}$ [9]. Here D is the electron diffusivity constant which is related to the electron mean free path, and thus resistivity, ρ. The Drude-Sommerfeld model[11] gives $D = \frac{v_F r_n^2}{\rho} \times 9.12 \cdot 10^{-17}$ for clean films, where v_F is the Fermi velocity and r_n is the Fermi radius parameter. For typical sputtered Au resistivities below 10 K ($\rho = 1\text{x}10^{-8}$ Ω·m, $D = 0.12$ m^2/s), ε_n can approach micron-sized dimensions ($\varepsilon_n \sim 1\mu$m at 150 mK), comparable to the dimensions of an optimized THM.

In this paper we present measurements of the transition behavior of THM test devices on the micron-size scale. We find evidence of a dramatic lateral proximity effect on the scales necessary for photon-noise-limited performance. These measurements corroborate previous measurements of similar TES devices at these scales[10]. In the final section we briefly discuss modifications to the design that would allow us to obtain a low T_c within the lateral proximity effect size regime.

TRANSITION MEASUREMENTS

Test Devices

We have fabricated antenna-coupled THM test devices optimized for CMB observations[4]. These devices consist of a 1.2 µm thick, 3 µm x 6 µm, 20 Ω evaporated Bi absorber which terminates a 20 Ω, 3 µm-wide Nb microstrip line. The microstrip line couples to a double slot antenna to allow illumination by a microwave source. The absorber overlaps a Mo/Au TES with superconducting Nb leads.

These devices were fabricated at the NASA-Goddard Detector Development Laboratory. The Mo/Au bilayers were deposited by sputtering. The Au TES pad was then etched using an ion-milling process, followed by RIE-etching of the Mo pad. This Mo pad extends out from the Mo/Au TES bilayer providing one of two avenues for contact to the Nb leads, as depicted in Figure 2a. The Nb leads and microstrip were deposited over the TES and then RIE-etched to obtain a sloped Nb sidewall for good step coverage by the absorber. The Bi absorber was deposited using a liftoff procedure and overlaps both the Nb microstrip line and TES as shown in Figure 1.

We fabricated TES test devices with two different bilayer thicknesses, 55nm Mo/350 nm Au and 65 nm Mo/350 nm Au. For lowest noise performance the smallest TES area is 3 µm x 3 µm square. We also fabricated TES devices with areas of 6 µm x 6 µm, 12 µm x 12 µm and 24 µm x 24 µm. As is visible in Figure 2b, the actual lead-to-lead dimensions for the TES devices varied from device to device on the same wafer due to a fabrication issue in which the Nb leads were over-etched at the point of contact with the Au TES layer.

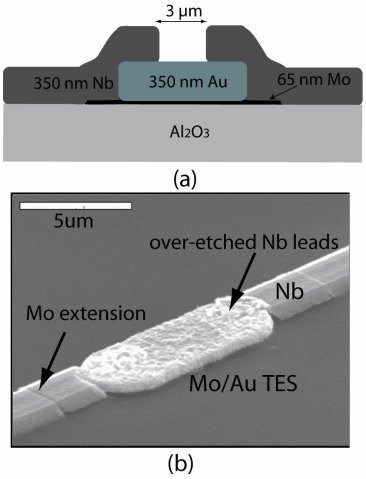

FIGURE 2. (a) A schematic of the contact between the Mo/Au TES and the Nb leads (b) An SEM image of the contact between the Nb leads and TES for a 3 µm x 3 µm device with no absorber or microwave circuit. The Mo layer which extends out from the TES is visible as a slight change in Nb thickness. The over-etching of the Nb leads on top of the Mo/Au TES is also clearly visible.

Resistance vs. Temperature Measurements

The test devices were cooled to 150 mK in a magnetically shielded ADR. 4-wire resistance vs. temperature measurements were taken using a lock-in amplifier to send a low amplitude (1.2 μA_{rms})

excitation current to the TES and to read out the TES voltage with an isolation-amplifer. We discovered that the TES transition temperature varied dramatically with the distance between the Nb lead contacts.

In Figure 3 the TES T_c as a function of lead-to-lead distance for the two different bilayers is plotted. The large uncertainties in lead-to-lead distance are due to the variation in Nb over-etching. As seen in Figure 3, we begin to see a dramatic shift towards higher T_c with lead-to-lead distances $\leq 12\mu m$. In fact, with some of the nominal 3 μm x 3 μm devices we find that the transition temperature has shifted to the base of the Nb transition near 8 K.

We have plotted a curve that is fit to this data (based on a relationship found for resistance vs. temperature measurements of similar Mo/Au TES devices with Nb leads[10]) following the form $T_c = T_{c0}\left(1+\left(\frac{L_0}{L}\right)^n\right)$. Here L is the lead-to-lead distance and L_0 is the characteristic distance scale at which we see a shift in the T_c. We find our measurements follow this trend but with large scatter at short distances, possibly due to the variation in actual lead-to-lead distance and/or variation in the quality of the Nb contact with the TES. A best fit, however, is provided by L_0 = 11-13 μm and n = 4-6.

We also find that the width of the transition increases with decreasing L. In some of smallest devices the transition is shifted so close to the Nb transition that the true transition and transition width for the TES become difficult to determine.

Resistance vs. temperature curves for two of the test devices are shown in Figure 4. The transition temperature, normal resistance and the transition width for all of the individual devices are listed in Table 1.

DISCUSSION

With the current Mo/Au thicknesses for the bilayer TES we find that the lateral proximity effect limits us to devices of lengths ≥ 12 μm if we are to retain a transition temperature within ~200 mK of the bulk T_c. In addition to shifting the T_c and increasing thermal noise, the proximity effect will also increase the SQUID amplifier noise by broadening the transition and decreasing the responsivity of the device.

There are several steps we can take to minimize the lateral proximity effect. These include using thinner and more resistive Au films to reduce the normal metal coherence length and to decrease the electron-phonon thermal conductance. Another possibility is to change the nearby lead material to one with a lower energy gap and transition temperature.

In our case, modifying the Mo/Au bilayer thickness is constrained due to lower limits on the Mo thickness required to obtain accurate transition temperatures. To avoid this bilayer limit we may need to use a single layer of Au for the TES, and make use of the Nb lateral proximity effect to obtain a reasonable transition temperature. Alternatively, pushing to lower operating temperatures can allow us to obtain a low noise for longer devices.

We are in the process of fabricating new devices to investigate the redesign options mentioned here and to further probe our understanding of this proximity effect. We are optimistic that one, or a combination of these design modifications, will allow us to obtain a micron-sized photon-noise-limited THM

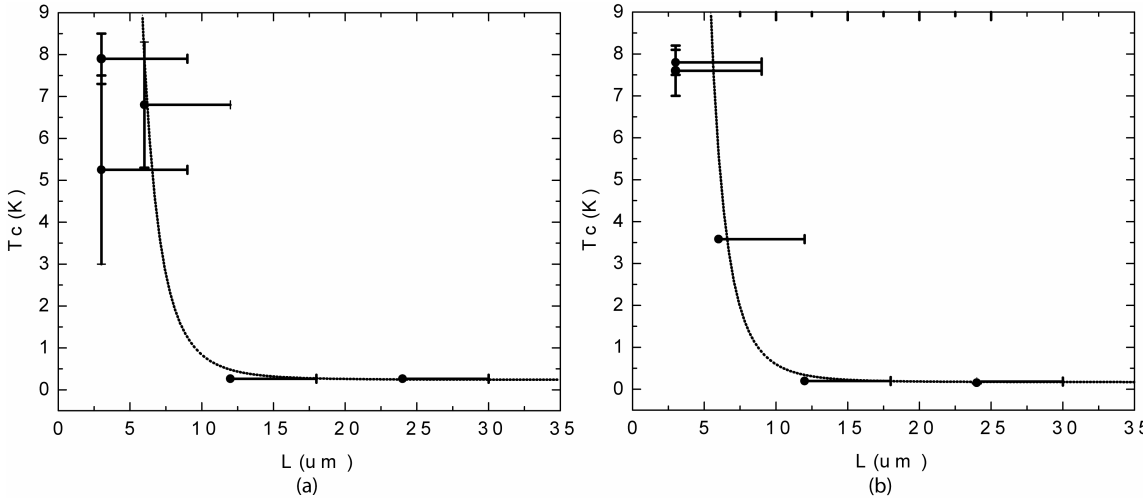

FIGURE 3. (a) T_c vs. lead-to-lead distance, L, for the 65 nm Mo/350 nm Au bilayer devices. A fit is shown for the parameters T_{c0} = 240 mK, L_0=12 μm and n = 5. (b) T_c vs. lead-to-lead distance, L, for the 55 nm Mo/350 nm Au bilayer devices. A fit is shown for the parameters T_{c0} = 170 mK, L_0 = 12 μm and n = 5. Data points indicate nominal L values while the error bars indicate variation due to over-etching. Error bars for T_c indicate uncertainty distinguishing the TES from the Nb lead transition.

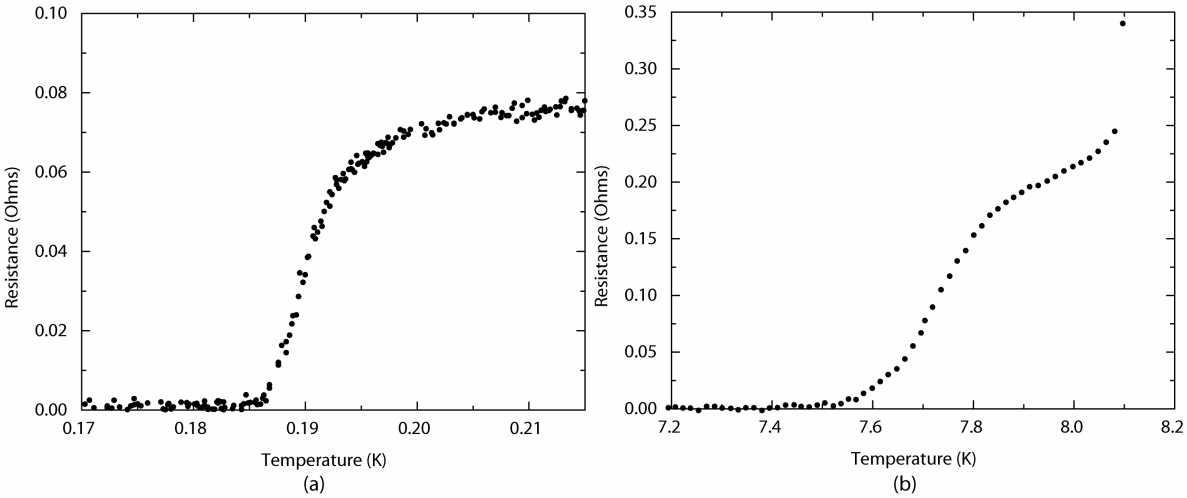

FIGURE 4. Resistance vs. temperature curves for two of the THM test devices. (a) Nominal 12 μm x 12 μm, 55 nm/350 nm thick, Mo/Au TES with absorber. (b) Nominal 3 μm x 3 μm, 55 nm/350 nm thick Mo/Au TES with absorber with a transition near the Nb lead transition.

TABLE 1. Transition measurements for individual test devices. Transition width, ΔT_c, was measured as the width between 10% and 90% of the normal resistance. T_c was measured as the midpoint between 10% and 90% normal resistance. For smaller devices the transition temperature and breadth could not be determined in this manner and limits are given instead. Most devices have an overlapping 3 μm wide Bi absorber.

Lead to lead length, L (μm)	Mo/Au Thickness (nm)	T_c (K)	ΔT_c (K)	Normal resistance (Ohms)	Absorber?
1977	65/350	0.243	0.007	13.82	no
24-30	65/350	0.263	0.010	0.033	yes
12-18	65/350	0.264	0.012	0.067	no
12-18	65/350	0.253	0.008	0.038	yes
6-12	65/350	≥5.4	≤3	-	yes
3-9	65/350	≥2.0	≤6	-	yes
3-9	65/350	7.3-8.5	≤1.2	-	yes
24-30	55/350	≤.240	≤.2	-	yes
12-18	55/350	0.193	0.012	0.078	no
6-12	55/350	3.58	0.760	0.214	yes
3-9	55/350	7.6-8.1	≤.5	-	yes
3-9	55/350	7.0-8.2	≤1.2	-	yes

ACKNOWLEDGEMENTS

We would like to thank D. McCammon and J. E. Sadleir for helpful discussions and advise. EB would also like to thank the NASA-Goddard GSRP Program for support.

REFERENCES

1. W. Hu and S. Dodelson, *Annu. Rev. Astron. And Astrophys*. vol. 40, pp. 171-216, September, 2002.
2. J. Wei et al., Nature Nanotech., vol. 3, p.496-500, August, 2008.
3. F. C. Wellstood, C. Urbina, and J. Clarke, *Phys. Rev. B* , vol. 49, pp. 5942-5955, March, 1994.
4. E. M. Barrentine et al., *J. of Low Temp. Phys.,* vol. 51, pp. 173-179, January, 2008.
5. E. M. Barrentine et al., *IEEE Trans. on Appl. Supercond*., Special Issue from the Applied Superconductivity Conference, submitted for publication, 2009.
6. J. M. Martinis et al., *Nucl. Instrum. Methods in Phys. Res., Sect. A*, vol. 444, pp 23-27, April, 2000.
7. S. Gueron, Ph.D thesis of CEA Saclay, 1998.
8. P. G. de Gennes, *Rev. Mod. Phys*., vol. 36, pp. 225-237, January, 1964.
9. K.K. Likharev, *Rev. Mod. Phys*., vol. 51, pp. 102-159, January, 1979.
10. J. E. Sadleir et al., oral presentation at Applied Superconductivity Conference, Chicago, August, 2008.
11. N. W. Ashcroft and N. D. Mermin, *Solid State Physics*, Saunders College, 1976, pp. 52.